ChemPhysChem

Chemistry Europe
European Chemical Societies Publishing

Accepted Article

Title: Reactivity of cobalt-fullerene complexes towards deuterium

Authors: Jan Vanbuel, Estefanía Germán, Guillaume Libeert, Koen Veys, Janni Moens, Julio A. Alonso, Maria López, and Ewald Janssens

To be cited as: *ChemPhysChem* 10.1002/cphc.202000146

Link to VoR: https://doi.org/10.1002/cphc.202000146

WILEY-VCH

WILEY-VCH

ARTICLE

Reactivity of cobalt-fullerene complexes towards deuterium

Jan Vanbuel,[a] Estefanía Germán,[b] Guillaume Libeert,[a] Koen Veys,[a] Janni Moens,[a] Julio A. Alonso,[b,c] María J. López,*[b] and Ewald Janssens**[a]

[a] Dr. J. Vanbuel, G. Libeert, K. Veys, J. Moens, Prof. Dr. E. Janssens
Quantum Solid State Physics, Department of Physics and Astronomy
KU Leuven
3001 Leuven, Belgium
**E-mail: ewald.janssens@kuleuven.be
[b] Dr. E. Germán, Prof. Dr. J. A. Alonso, Prof. Dr. M. J. López
Departamento de Física Teórica, Atómica y Óptica
Universidad de Valladolid
47011 Valladolid, Spain
*E-mail: maria.lopez@fta.uva.es
[c] Prof. Dr. J. A. Alonso
Donostia International Physics Center
20018 San Sebastián, Spain

Supporting information for this article is given via a link at the end of the document.

Abstract: The adsorption of molecular deuterium (D_2) onto charged cobalt-fullerene-complexes $Co_nC_{60}^+$ (n = 1 – 8) is measured experimentally in a few-collision reaction cell. The reactivity is strongly size-dependent, hinting at clustering of the transition metals atoms on the fullerenes. Formation and desorption rate constants are obtained from the pressure-dependent deuterogenation curves. DFT calculations indeed find that this transition metal clustering is energetically more favorable than decorating the fullerene. For n = 1, D_2 is predicted to bind molecularly and for n = 2 dissociative and molecular configurations are quasi-isoenergetic. For n = 3 – 8, dissociation of D_2 is thermodynamically preferred. However, reaching the ground state configuration with dissociated deuterium on the timescale of the experiment may be hindered by dissociation barriers.

Introduction

Ever since their discovery in 1985[1] and their production in large quantities via the Kratschmer-Huffman carbon arc method,[2] fullerenes have taken center stage in contemporary chemical and physical research. Besides having interesting intrinsic properties, additional tunable degrees of freedom can be achieved by decorating fullerenes and substituting carbon atoms with other atoms, as well as incorporating foreign species inside the fullerene cage.[3-5] Doping C_{60} with alkali atoms, for example, results in the formation of correlated electron systems exhibiting both superconductivity and magnetism.[6,7] Cobalt doped fullerenes have been suggested as catalysts for single walled carbon nanotube formation of uniform diameter.[8,9]

Fullerenes are also considered ideal model systems for porous carbon materials, which are attractive for hydrogen storage due to their high surface area.[10-12] Because hydrogen is physically adsorbed to these materials, cryogenic cooling is needed to reach a volumetric energy density useful for practical applications. Computational studies indicate that the binding strength can be enhanced by decorating fullerenes with transition metals or alkali metals.[13-16] Although the theoretical hydrogen weight percentages are impressive (almost 9 wt% for Sc and Ca), some of these findings are questioned by calculations that predict clustering of the transition metal atoms,[17,18] which would drastically lower the maximal amount of adsorbed hydrogen.

Experimental studies of transition metals adsorption on fullerenes, however, provide no clear-cut answer to the question of clustering/decoration. Mass spectrometric work on $M_nC_{60}^+$ (M = Ca, Ba, Sr, n = 0 – 500)[19,20] and $TM_nC_{60}^+$ (TM = Ti, Zr, V, Y, Ta, Nb, n = 0 – 150)[19,20] by the group of T.P. Martin, provided evidence for (transition) metal coating of the fullerenes at high coverages, i.e. $n \geq 32$, but could not draw conclusions for $n < 32$. Fye and Jarrold found, using ion mobility measurements, that niobium atoms may cluster together on the fullerene surface, and some atoms might even enter the fullerene cage.[21] Parks et al. probed the interaction of Ni_n (n = 2 – 72) clusters with fullerenes in a flow-tube reactor and found no sign of fullerene decomposition upon complexation, even at elevated temperatures.[22] Duncan and coworkers concluded from photodissociation experiments of TMC_{60}^+ complexes (TM = Fe, V, Co) that by changing growth conditions, clustered, dispersed, and even inserted transition-metal-fullerene complexes could be produced.[23]

A second aspect of relevance within the context of hydrogen storage is the hydrogen binding geometry, i.e. whether hydrogen binds dissociatively or molecularly. Work in the group of R.E. Smalley showed that neutral cobalt clusters adsorb hydrogen dissociatively, albeit in a size-dependent way.[24] Nakajima and co-workers obtained similar results for cationic cobalt clusters,[25] indicating that a single electron does not significantly affect the size-dependency of the reactivity. In contrast to the dissociative hydrogen adsorption on neutral and cationic cobalt clusters, hydrogen is known to bind dissociatively to a neutral cobalt atom and molecularly to a cobalt cation[26]. Calculations predict that this molecular binding is also present if a single cobalt atom is supported by a fullerene, because the cobalt atom becomes partially positively charged due to a charge transfer to the fullerene .[13]

In the current work, we studied the reaction kinetics of laser ablated cobalt doped fullerenes, $Co_nC_{60}^+$ (n = 1 – 8), with D_2 in a few-collision reaction cell. Molecular deuterium (D_2) was used for mass spectrometric reasons. Density functional theory (DFT) calculations were used to gain insight into the geometry of both

cobalt-fullerene complexes and molecular hydrogen (H_2) binding, as well as the size-dependence of the energy landscape of H_2 adsorption. The results of the DFT calculations do not distinguish between different isotopes of hydrogen and can therefore be compared with the experimental results.

Results and Discussion

Experimental results

Cobalt-fullerene complexes, $Co_nC_{60}^+$ (n = 1 – 8), are produced in a laser ablation source and expansion into vacuum yields a beam of particles that flies through a reaction cell containing D_2 at a pressure of 0 – 0.3 Pa. In the reaction cell, both formation of the deuterogenated complexes (with rate constant k_F) and desorption of D_2 (with rate constant k_D) take place (equation 1), whereas only desorption occurs after the clusters exit the reaction cell (equation 2):

$$\mathrm{TM}_n\mathrm{C}_{60}^+ + \mathrm{D}_2 \overset{k_F}{\rightarrow} (\mathrm{TM}_n\mathrm{C}_{60}\mathrm{D}_2)^+ \overset{k_D}{\rightarrow} \mathrm{TM}_n\mathrm{C}_{60}^+ + \mathrm{D}_2 \quad (1)$$

$$(\mathrm{TM_nC_{60}D_2})^+ \overset{\mathrm{k_D}}{\rightarrow} \mathrm{TM_nC_{60}^+} + \mathrm{D_2} \quad (2)$$

Due to the low pressure in the reaction cell (0 – 0.3 Pa), the rate constants can be considered time-independent. The fraction of deuterogenated complexes $F(\mathrm{D}_2)$ that arrive at the detector is given by[27]

$$F(\mathrm{D}_2) = \frac{k_F.p_{D2}}{k_F.p_{D2} + k_D k_B T}\, e^{-k_D t_2}\left(1 - e^{-\left(k_F\frac{p_{D2}}{k_B T} + k_D\right)t_1}\right), \quad (3)$$

with p_{D2} the D_2 pressure in the reaction cell, T the reaction cell temperature (= 293 K) and t_1 and t_2 the (fixed) times the clusters spend in the reaction cell and between the reaction cell and the TOF-MS extraction, respectively.

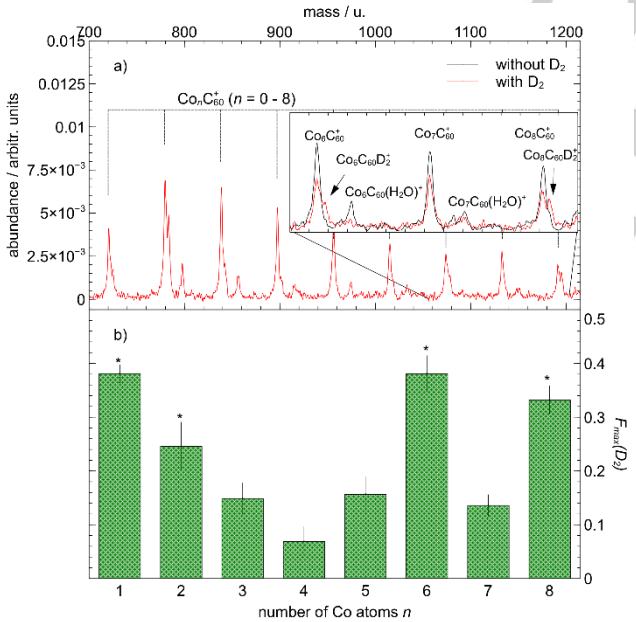

Figure 1. a) Representative mass spectrum of deuterogenated $Co_nC_{60}^+$ (n = 1 – 8) clusters. The inset present a zoom of the n = 6 – 8 size range and compares the mass spectrum without (black) and with (red) D_2 in the collision cell. b) Maximal fraction of deuterogenated complexes, $F_{max}(\mathrm{D}_2)$, for $Co_nC_{60}^+$ (n = 1 – 8) clusters. The reactive sizes, for which the formation and desorption rates could be obtained quantitatively, are denoted with an asterisk

Table 1. Calculated hard sphere collision rate k_{HS}, fitted forward reaction rate k_F, ratio between the fitted forward reaction rates and the calculated Langevin reaction rate k_F/k_L, and fitted desorption rate k_D for $Co_nC_{60}^+$. For n = 1,2,6,8 two values are provided for k_D, corresponding to the value obtained from the fit assuming k_{HS} for the forward rate (one fit parameter, left value) and to the one obtained when fitting both k_F and k_D (right value).

n	k_{HS} (10^{-16} m^3/s^{-1})	k_F (10^{-16} m^3/s^{-1})	k_F/k_L	k_D (10^3 s^{-1})
1	2.3	11 ± 3	1.1 ± 0.3	5 ± 1 / 11 ± 1
2	3.0	7 ± 5	0.7 ± 0.5	11 ± 1 / 15 ± 3
3	3.5			18 ± 7
4	4.0			32 ± 3
5	4.4			21 ± 4
6	4.7	3 ± 1	0.3 ± 0.1	10 ± 1 / 8 ± 3
7	5.1			22 ± 5
8	5.4	3 ± 2	0.3 ± 0.2	12 ± 1 / 9 ± 3

Fig. 1a shows a mass spectrum of the Co_nC60^+ (n = 1 – 8) complexes after interaction with D_2 in the reaction cell at a pressure of 2.6 μbar. The inset presents a zoom of the n = 6 – 8 size range and compares the spectrum without (black) and with (red) D_2. Adsorbed water impurities can be seen in between the main Co_nC60^+ abundances. Asides from the cobalt cluster-fullerene complexes, no cobalt clusters are seen in the mass spectra. This suggests a similar formation mechanism to that proposed by Grieves et al.[23], i.e. under the present experimental condition (gas pressure, laser power, timing) complexes grow by successive addition of metal atoms onto the fullerene. Figure 1b shows the maximal fraction of deuterogenated clusters $F_{max}(\mathrm{D}_2)$, i.e. the fraction of deuterogenated complexes at the highest pressure in the reaction cell ($p_{D2} = 0.3$ Pa), corresponding to an average of 1 – 2 collisions, for each $Co_nC_{60}^+$ (n = 1 – 8) cluster. Sizes n = 1, 2, 6 and 8 are clearly more reactive than sizes n = 3, 4, 5 and 7. Note that "reactive" within the timescale of the experiment (100 μs) implies either a high formation rate, a low desorption rate due to a high binding energy, or a combination of both. An "unreactive" cluster is similarly defined. The reactivity is found to be strongly size-dependent. This strong size-dependence indicates that the transition metal atom cluster together on the fullerene. In the case the metal atoms would decorate the fullerene, one would expect a smooth size dependence related to the charge transfer between the metal atoms and the fullerene.

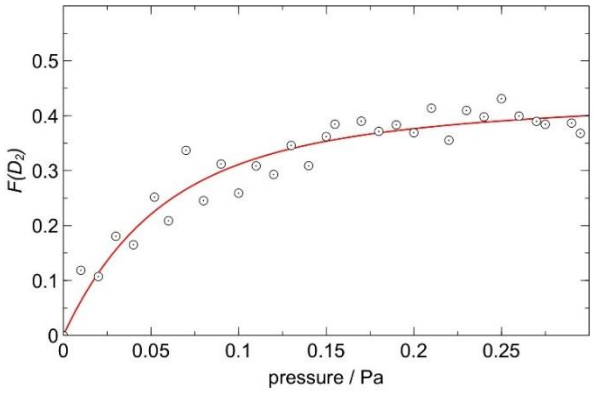

Figure 2. Pressure-dependent deuterogenation curve of CoC_{60}^+

For the reactive sizes *n* = 1, 2, 6 and 8, which are denoted in Fig. 1b with an asterisk, pressure-dependent deuterogenation curves were fitted with equation (3) to obtain quantitative values for k_F and k_D. An example of such a curve and its corresponding fit is shown for *n* = 1 in Fig. 2. The curves and fits for *n* = 1 – 8 are provided as Fig. S1 in the supporting information (SI). For *n* = 3, 4, 5 and 7, fit uncertainties when fitting both parameters were too large to be meaningful. For these sizes, we therefore assumed a hard sphere collision cross section so that the only fit parameter was the desorption rate k_D. The results are tabulated in Table 1. The correspondence between k_D values obtained using both approaches, indicates that the assumption of a hard sphere collision cross section made for the forward rate has a limited influence on the extracted desorption rate. The exception is the difference in the k_D values for *n* = 1, which can be explained by the bad approximation of k_{HS} for k_F in this specific case.

Table 1 contains, besides the fitted k_F and k_D values, also the hard sphere collision rate k_{HS} defined as

$$k_{HS} = S \cdot \sigma_{geom}\, v_{rel} = S\, \pi \left(R_{\mathrm{Co}_n} + R_{\mathrm{D}_2}\right)^2 v_{rel}, \qquad (4)$$

with S a steric factor accounting for the fact that approximately 20% of the clusters' entire solid angle is blocked by the fullerene (see details in the supporting information), $R_{\mathrm{Co}_n} = r_{\mathrm{Co}} n^{1/3}$ the radius of a spherical *n*-atom cobalt cluster, R_{D_2}= 0.74 Å the bond length of the deuterium molecule, and $v_{rel} \approx$ 1500 m/s the average relative velocity between cluster beam and deuterium molecules in the reaction cell. Column k_F/k_L compares the forward reaction rates with the Langevin formation rates $k_L = \sigma_L v_{rel}$, with σ_L the cross section determined by the ion-induced dipole interaction between cluster and deuterium molecule. σ_L is given by[28]

$$\sigma_L = \frac{e}{4\epsilon_0}\left(\frac{2\alpha}{E_{CM}}\right)^{\frac{1}{2}}, \qquad (5)$$

with α the perpendicular polarizability of D_2 and E_{CM} the kinetic energy in the center-of-mass frame of the cluster and the deuterium molecule. The fitted forward rate for *n* = 1 and 2 is closer to the Langevin rate than to the hard sphere collision rate. For larger sizes, the formation rate is closer to and even smaller than the hard sphere collision rate.

Whether the D_2 adsorbs dissociatively or molecularly cannot be deduced directly from the experimental reaction rates. In principle there are three possibilities: 1) the D_2 weakly physisorbs, 2) the D_2 adsorbs molecularly, but more strongly than physisorbed D_2, via a charge-induced dipole or Kubas-type of interaction, or 3) D_2 dissociates upon adsorption. The first possibility, physisorption, is unlikely; physisorbed complexes are too weakly bound to survive during the time the complexes travel between the reaction cell and the extraction zone of the TOF-MS (≈ 50 µs) at the experimental temperature (*T* = 293 K). For the larger sizes, it is also unlikely that charge localization is enough to cause a strong charge-induced dipole interaction, leaving the options of dissociative adsorption and Kubas-complexation. As Kubas complexes are more common for low-coordination numbers, dissociative adsorption seems to be the most likely explanation. Experimental and computational studies on free cobalt clusters in literature also suggest that hydrogen/deuterium adsorbs dissociatively.[24,29] Although collision-induced dissociation experiments found no significant energy barriers towards hydrogenation,[30] dissociative adsorption of H_2 is often site-specific.[31] A dependence of the forward rate on the initial encounter site could for the larger clusters (*n* = 6, 8) explain why the fitted k_F values are significantly smaller than the Langevin cross section, and even smaller than the hard sphere geometric cross section.

Computational results

Bare $Co_nC_{60}^+$ (n = 1 – 8) complexes

To further corroborate these hypotheses, we performed density functional theory calculations. In Fig. 3 side and top views of the lowest energy geometries obtained for $Co_nC_{60}^+$ with *n* = 1 – 8 are presented. The first three cobalt atoms adsorbed on the fullerene are in direct contact with the carbon atoms of the fullerene surface, forming a triangle parallel to a hexagon of the fullerene. Additional cobalt atoms attach to the previous ones, resulting in three dimensional clusters: a trigonal pyramid for *n* = 4, a trigonal bipyramid for *n* = 5, an octahedron for *n* = 6, a pentagonal bipyramid for *n* = 7 and a bicapped octahedron for *n* = 8. All three-dimensional clusters are supported on a triangular Co_3 base lying parallel to a hexagon of the fullerene. The possibility of Co island formation (wetting the surface of the fullerene) was also considered, but those structures were either higher energy configurations (less stable) or reconstructed to 3D geometries.

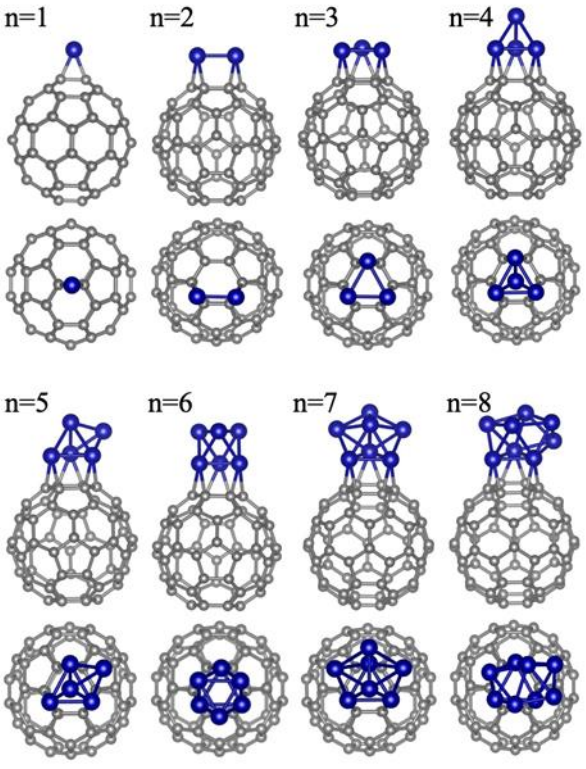

Figure 3. Lowest energy structures of $Co_nC_{60}^+$ (*n* = 1 – 8) clusters. Each panel contains a side view (upper structure) and a top view of the complex (lower structure). For all sizes, the cobalt atoms cluster together rather than decorating the fullerene cage. The cobalt atoms are blue, the carbon atoms grey.

Although the lowest energy structures presented in Fig. 3 indicate cobalt clustering on the fullerene, possible decoration deserves careful consideration. To this purpose, successive adsorption of cobalt atoms on the C_{60} fullerene was investigated.

Table 2 contains the binding energies E_B(Co,n) of the last cobalt atom in $Co_nC_{60}^+$, defined as:

$$E_B(\mathrm{Co}, n) = E(\mathrm{Co}_{n-1}\mathrm{C}_{60}^+) + E(\mathrm{Co}) - E(\mathrm{Co}_n\mathrm{C}_{60}^+), \qquad (6)$$

where $E(Co_nC_{60}^+)$ is the energy of the Co_n–fullerene complex and E(Co) the energy of an isolated cobalt atom in the cubic supercell. For the smallest $Co_1C_{60}^+$ complex, alternatively the binding energy of the Co^+ cation on neutral C_{60} is calculated because most fullerenes in the experiment are expected to be neutral, i.e:

$$E_B(\mathrm{Co}^+, 1) = E(\mathrm{C}_{60}) + E(\mathrm{Co}^+) - E(\mathrm{CoC}_{60}^+). \qquad (7)$$

The adsorption energy of Co^+ on neutral C_{60} is substantially larger (3.70 eV) than that of Co on $Co_1C_{60}^+$ (3.11 eV). We therefore explored the option that cobalt atoms decorate the fullerene. It was found that a second (neutral) cobalt is stronger bound in the vicinity of the first pre-adsorbed Co atom than to any other fullerene site far from this pre-adsorbed Co (3.11 eV vs. 1.99 eV, see Fig. S3 in the SI). A second possibility that a priori cannot be ruled out is that the fullerene is not decorated with atoms, but with small Co clusters instead of one large cluster. Since it is computationally unfeasible to do a full combinatorial optimization, we restrict ourselves to two examples that are provided in the SI. For both $Co_5C_{60}^+$ and $Co_6C_{60}^+$, formation of single Co_5 and Co_6 clusters on the fullerene surface is energetically preferred to combining Co_2 and Co_3. This predicted clustering is in good agreement with other computational studies on transition metal cluster-fullerene complexes, such as those by Méndez-Camacho and Guirado-López for Pt_nC_{60}[32] and by Sun et al. for Ti_nC_{60}.[18] It therefore seems that the global minimum on the PES is the configuration in which the transition metal atoms cluster together. Nevertheless, the question whether this global minimum can be achieved experimentally is non-trivial and the answer likely depends on the growth process conditions of the transition-metal-fullerene complex, cfr. ref.[23].

Table 2: Binding energies $E_B(\mathrm{Co}, n)$ of the last Co atom in $Co_nC_{60}^+$ (n = 1 –8), defined in eq. (6), and adsorption energies for molecular, $E_{ads}(\mathrm{H}_2)$, and dissociated, $E_{ads}(2\mathrm{H})$, hydrogen adsorption on $Co_nC_{60}^+$ (n = 2 – 8). For $Co_1C_{60}^+$, alternatively the binding energy of Co^+ on C_{60}, defined in eq. (7), is listed (right value).

n	$E_B(\mathrm{Co}, n)$ (eV)	$E_{ads}(\mathrm{H}_2)$ (eV)	$E_{ads}(2\mathrm{H})$ (eV)
1	2.52 / 3.70	1.06	---
2	3.11	1.19	1.16
3	4.19	0.60	1.05
4	4.13	0.68	1.54
5	3.68	0.74	1.60
6	4.22	0.59	1.15
7	4.31	0.63	1.29
8	3.90	0.84	1.48

Hydrogenated $Co_nC_{60}^+$ (n = 1 – 8) complexes

To better understand the interaction of cobalt-fullerene complexes with molecular hydrogen, the $Co_nC_{60}^+$ (n = 1 – 8) complexes from figure 3 were allowed to react with both molecular and dissociated H_2 to form $(Co_nC_{60}H_2)^+$ and $(Co_nC_{60}2H)^+$, respectively. Their optimized structures are depicted in Fig. 4. The hydrogen molecule attaches on top of one of the Co atoms in direct contact with the fullerene for n = 1 – 4, whereas it binds on top of a Co atom not in contact with the fullerene for n = 6 – 8. For n = 5, the hydrogen molecule binds between one cobalt of the triangular face in contact with the fullerene and a Co atom not directly in contact. For sizes n = 2 – 5 and 8, the dissociated hydrogen atoms bridge two cobalt atoms. For n = 6, one of the hydrogen atoms bridges a Co–Co edge, whereas the other binds to a triangular face of the Co cluster. For n = 7, both hydrogen atoms bind to triangular faces of the Co cluster. García-Díez et al. computationally studied the adsorption of H_2 on Co_6 and Co_{13}.[29] In their study similar adsorption sites were found as for the cobalt-fullerene complexes: molecular hydrogen on top of a Co atom, and the hydrogen atoms of a dissociated molecule on Co-Co edges.

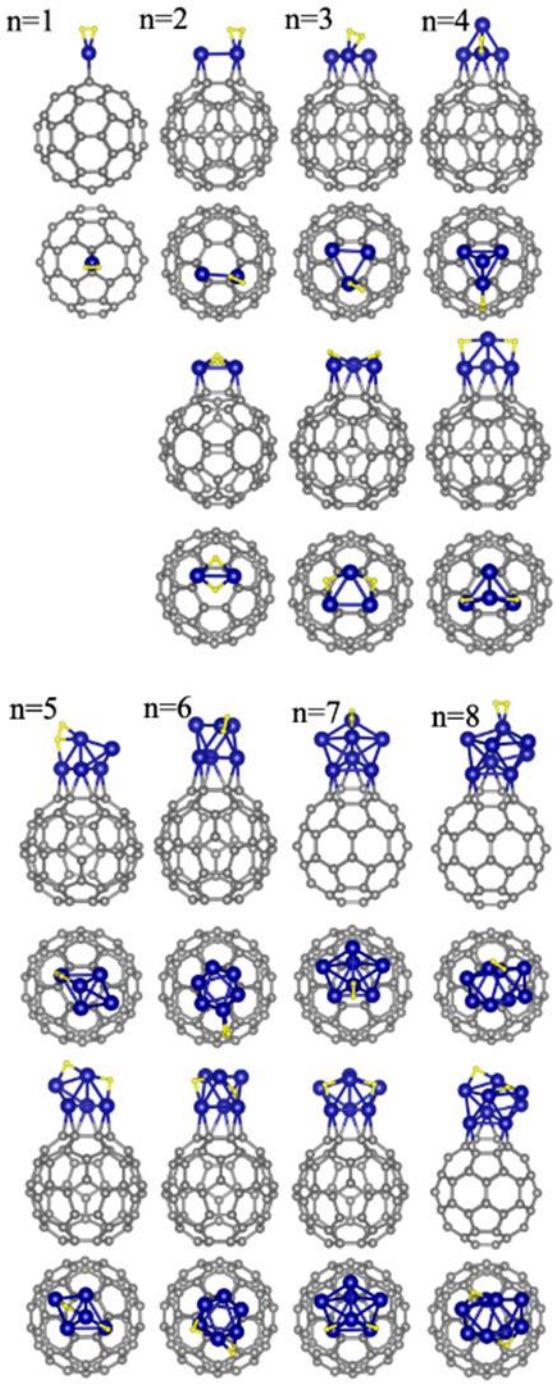

Figure 4. Lowest energy structures of $(Co_nC_{60}H_2)^+$ (n = 1–8) clusters (rows 1,2 and 5,6) and lowest energy structures of $(Co_nC_{60}2H)^+$ (n=2–8) clusters (rows 3,4 and 7,8). Side (upper structure) and top (lower structure) views of the complexes are given. Cobalt atoms are blue, carbon atoms grey and hydrogen atoms yellow.

The molecular adsorption energy $E_{ads}(H_2)$ as well as the dissociative adsorption energy $E_{ads}(2H)$ of H_2 were calculated, and defined as:

$$E_{ads}(H_2) = E(Co_nC_{60}^+) + E(H_2) - E((Co_nC_{60}H_2)^+) \quad (8)$$

and

$$E_{ads}(2H) = E(Co_nC_{60}^+) + E(H_2) - E((Co_nC_{60}2H)^+, \quad (9)$$

respectively. The calculated values are listed in table 2. See Table TS1 of the SI for the spin magnetic moments of all investigated $Co_nC_{60}^+$ (n = 1 – 8) complexes, before and after adsorption of molecular or dissociated H_2.

For n = 1, only molecular adsorption is exothermic. This is in agreement with computational work by Zhao et al. for hydrogen adsorption on complexes of C_{60} with a single metal atom, predicting dissociative adsorption for the lightest transition metals, such as Sc and V, and molecular adsorption for heavier transition metals, including Co.[13] For n = 2, molecular and dissociative adsorption are both possible as the respective binding energies differ only 30 meV in favor of molecular adsorption. For n = 3 – 8 dissociative chemisorption is energetically preferred to molecular adsorption. A similar trend can be observed for both the molecular and dissociative adsorption energies: there is an increase from n = 3 to n = 5, a local minimum at n = 6, and a further increase for n = 7 and 8.

Our calculations predict that the dissociative adsorption energies are highest for n = 4 and n = 5. Notably, for free cationic cobalt clusters, Nakajima et al.[25] also found that sizes n = 4 and n = 5 are the most reactive clusters smaller than 10 atoms, not only towards hydrogen but also towards other reactants such as methane and ethylene. Similarly, Gehrke et al.[33] calculated that the Ar binding energy to Co_n^+ (n = 4 − 8) clusters is largest for Co_4^+ and Co_5^+, which explained why these sizes were more readily taggable by argon than others. Higher calculated molecular and dissociative H_2 adsorption energies of $Co_4C_{60}^+$ and $Co_5C_{60}^+$, with respect to neighboring sizes, therefore suggest that the interaction of hydrogen with the cobalt cluster−fullerene complexes is similar to that of free cobalt clusters, or, put differently, that the effect of the fullerene support on the reactivity of the cobalt clusters is limited.

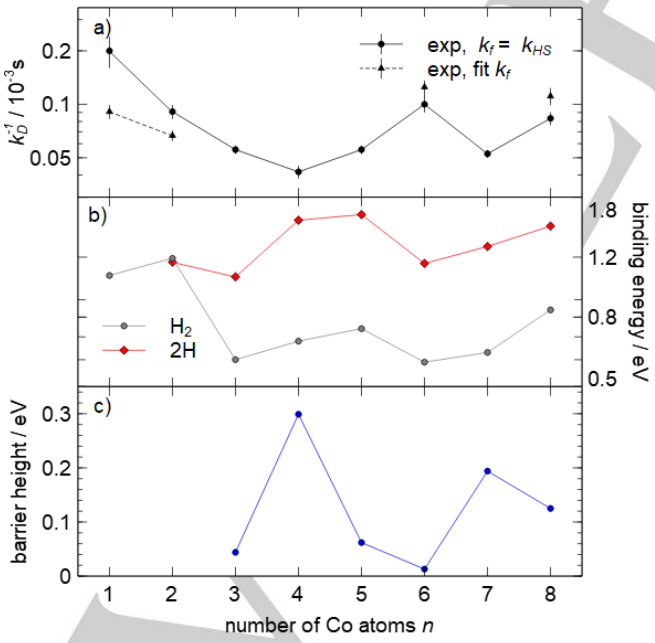

Figure 5. a) Inverse of the experimental desorption rates. b) Calculated adsorption energy of the H_2 molecule and chemisorption energy of the dissociated molecule. c) Calculated barrier heights for H_2 dissociation on the supported Co_n (n = 3–8) clusters.

Discussion

The experimental and simulated results are compared in Fig. 5. Fig. 5a contains the inverse of the experimental desorption rates. The error bars correspond to propagated errors of the fitted k_D rates under the assumption of a hard-sphere collision cross section (circles, full line) and error bars obtained by fitting both reaction rates (triangles, dotted line). Although the absence of a buffer gas in the reaction cell renders temperature an ill-defined concept and would strictly require the use of the microcanonical ensemble, often an Arrhenius-type rate fits the data well.[34] One would therefore expect k_D^{-1} to correlate with the adsorption energy.

However, at first sight there is no clear correlation between the k_D^{-1} values in Fig. 5a and the calculated adsorption energies in Fig. 5b. Whereas k_D^{-1} is maximal for n = 6, both the molecular and dissociative adsorption energies have a local maximum at n = 5. In addition, the least reactive clusters in the experiment are n = 4 and n = 7, but the calculations predict that the H_2 complexes are least strongly bound for n = 3 and n = 6.

For n = 3–8 the dissociative H_2 adsorption energies (1.05–1.60 eV) are significantly higher than molecular adsorption energies (0.55–0.84 eV). The relatively high experimental k_D values (of the order of 10^4 s^{-1}) hint that reaching the dissociative chemisorption on the timescale of the experiment is not a given. For example, if one applies an RRKM model for $Co_4C_{60}^+$ and assumes that the H_2 binding energy of 1.5 eV is fully redistributed over the cluster-fullerene complex, which was initially at room temperature, H_2 desorption rates of 1–10^{-4} s^{-1} are found (depending on the assumptions for the dissociation process). This order of magnitude estimate indicates that the high experimental desorption rates are caused by desorption of D_2 from the less strongly bound adsorption complexes and thus not all (or maybe even none) of the complexes reach the strongly bound dissociative state.

In the collision cell, D_2 molecules collide with the $Co_nC_{60}^+$ complex and a $(Co_nC_{60}D_2)^+$ encounter complex can be formed. The bonding strength of this encounter complex is likely relevant for the experimental forward rate k_f. The calculated high molecular binding energies for n = 1 and 2 are in line with the high fitted k_f rates for these sizes. For the larger n = 3–8 sizes the molecular complex is not the lowest energy configuration. The dynamics before reaching the dissociated complex may determine the measured desorption rates, since no desorption is expected from the strongly bound dissociated complexes. The average time to reach the dissociated D_2 complex depends on the magnitude of the activation barriers along the D_2 dissociation pathway. Those modelled barriers for H_2 are plotted in Fig. 5c for n = 3–8 (the sizes that have dissociated H_2 in the lowest energy configuration). Note that all barriers are below 0.5 eV and thus below the molecular adsorption energy, i.e. the energy gained during the initial adsorption, so dissociation of D_2 should be possible. However, the relative large fullerene acts as a heat bath and the

time to cross the barrier may be much longer than the timescale of the experiment (100 μs). There is indeed an anti-correlation between the barrier height and k_D^{-1}. In particular, the very low calculated H_2 dissociation barrier for $Co_6C_{60}H_2$ of 0.013 eV indicated that deuterium dissociation in $Co_6C_{60}D_2$ is likely facile and the system may reach the ground state, explaining the low experimental k_D value for this size. Summarizing, this seems to confirm that a higher activation barrier implies the system remains (on average) longer in the molecular $(Co_nC_{60}D_2)^+$ complexes and thus D_2 desorption is more likely.

Conclusion

The adsorption of D_2 onto transition metal doped fullerenes $Co_nC_{60}^+$ (n = 1 – 8) was measured in a few-collision reaction cell. The reactivity is strongly size-dependent, indicating transition metal clustering on the fullerene. By fitting the pressure-dependent deuterogenation curves of the complexes, quantitative values of the formation rate constant k_F and desorption rate constant k_D were obtained. For n = 1 and 2, the forward reaction rate agrees well with a Langevin rate (ion-induced dipole interaction). For n = 6 and 8, k_F is significantly smaller and points in the direction of the sterically more demanding process of dissociative adsorption. DFT calculations support that clustering of the transition metals is indeed energetically more favorable than decorating the fullerene. For the cobalt monomer on a fullerene, the D_2 is predicted to bind molecularly and for the cobalt dimer dissociative and molecular adsorption energies are quasi-isoenergetic. For the larger n = 3–8 sizes, dissociative D_2 adsorption is energetically preferred. Comparison of the calculated H_2 adsorption energies with the experimental D_2 desorption rates indicates that reaching the ground state configuration with dissociated D_2 on the timescale of the experiment may be hindered by, relatively small, dissociation barriers.

Methods Section

The cobalt-fullerene complexes, $Co_nC_{60}^+$ (n = 1 – 8), are produced in a dual laser ablation source [35] and detected by time-of-flight mass spectrometry (TOF-MS). The fullerene target is prepared by cold-pressing C_{60} powder (Sigma Aldrich, 99.5% purity) at a pressure of approximately 1 – 2 kbar, similar to the procedure reported by Nakajima et al.[36] To avoid fragmentation of the fullerenes by laser ablation,[37] the target is evaporated by operating a 532 nm Nd-YAG laser in long pulse mode (200 μs pulse length instead of 6 ns in Q-switch mode). After production but before entering the extraction zone of the TOF-MS, the clusters fly through a few collision reaction cell containing D_2 at a pressure of 0 – 0.3 Pa, which has been described in more detail earlier.[38,39]

The electronic and structural properties of bare and hydrogenated $Co_nC_{60}^+$ systems were simulated by carrying out DFT calculations,[40] employing version 6.2.1 of the quantum-ESPRESSO suite of electronic structure codes.[41] The projector augmented wave method (PAW) accounts for the electron−ion core interaction[42,43] and the Perdew–Burke–Ernzerhof (PBE) functional[44] was employed for electronic exchange and correlation. A plane-wave cutoff energy of 40 Ry was used to expand the Kohn–Sham orbitals, and 350 Ry for the charge density. The studied systems were modeled in a cubic supercell of 17 x 17 x 17 Å^3, which is large enough to assure no interaction among periodic images. The Γ point for the Brillouin zone integration was employed in the calculation. The Grimme-D3 method was used to account for the dispersion correction in the density functionals.[45] More details about the convergence of the calculations are provided in the SI.

As the system is charged, the Makov-Payne correction was included.[46] This correction is applied to calculate the total energy of an isolated charged system (a molecule or a cluster in a 3D supercell) with periodic boundary conditions; the method also calculates an estimate of the vacuum level so that eigenvalues can be properly aligned.[46] The energy barriers and reaction pathways for the dissociation of H_2 adsorbed on $Co_nC_{60}^+$ have been calculated with the nudged elastic band (NEB) method.[47,48]

Acknowledgements

This work was supported by KU Leuven Research Council (C14/18/073). We also acknowledge support by Junta de Castilla y León (Grant VA021G18) and University of Valladolid (GIR Nanostructure Physics). The authors thankfully acknowledge the facilities provided by Centro de Proceso de Datos, Parque Científico (University of Valladolid). J.V. and E.G. acknowledge the Research Foundation Flanders (FWO) for a PhD fellowship and the University of Valladolid for a postdoctoral fellowship, respectively.

Keywords: fullerenes • metal clusters • hydrogen adsorption • mass spectrometry • density functional theory

[1] H. W. Kroto, J. R. Heath, S. C. O'Brien, R. F. Curl, R. E. Smalley, *Nature* **1985**, *318*, 162-163.

[2] W. Krätschmer, L. D. Lamb, K. Fostiropoulos, D. R. Huffman, *Nature* **1990**, *347*, 354-358.

[3] A. A. Popov, S. Yang, L. Dunsch, *Chem. Rev.* **2013**, *113*, 5989-6113.

[4] A. L. Balch, M. M. Olmstead, *Chem. Rev.* **1998**, *98*, 2123-2166.

[5] M. Robledo, N. F. Aguirre, S. Díaz-Tendero, F. Martín, M. Alcamí, *RSC Advances* **2014**, *4*, 53010-53020.

[6] A. F. Hebard, M. J. Rosseinsky, R. C. Haddon, D. W. Murphy, S. H. Glarum, T. T. M. Palstra, A. P. Ramirez, A. R. Kortan, *Nature* **1991**, *350*, 200-601.

[7] A. Y. Ganin, Y. Takabayashi, P. Jeglič, D. Arčon, A. Potočnik, P. J. Baker, Y. Ohishi, M. T. McDonald, M. D. Tzirakis, A. McLennan, *Nature* **2010**, *466*, 221-225.

[8] P. R. Birkett, A. J. Cheetham, B. R. Eggen, J. P. Hare, H. W. Kroto, D. R. M. Walton, *Chem. Phys. Lett.* **1997**, *281*, 111-114.

[9] C. H. Kiang, M. S. Devries, G. Gorman, R. Savoy, D. S. Bethune, J. Vazquez, R. Beyers, *Nature* **1993**, *363*, 605-607.

[10] A. C. Dillon, K. M. Jones, T. A. Bekkedahl, C. H. Kiang, D. S. Bethune, M. J. Heben, *Nature* **1997**, *386*, 377.

[11] I. Cabria, M. J. López, J. A. Alonso, *Carbon N. Y.* **2007**, *45*, 2649-2658.

[12] J. A. Alonso, I. Cabria, M. J. López, *J. Mater. Res.* **2013**, *23*, 589.

[13] Y. Zhao, Y. H. Kim, A. C. Dillon, M. J. Heben, S. B. Zhang, *Phys. Rev. Lett.* **2005**, *94*, 155504.

[14] A. Kaiser, M. Renzler, L. Kranabetter, M. Schwärzler, R. Parajuli, O. Echt, P. Scheier, *Int. J. Hydrog. Energy* **2017**, *42*, 3078-3086.

[15] T. Yildirim, S. Ciraci, *Phys. Rev. Lett.* **2005**, *94*, 175501.

[16] M. Yoon, S. Yang, C. Hicke, E. Wang, D. Geohegan, Z. Zhang, *Phys. Rev. Lett.* **2008**, *100*, 1-4.

[17] P. O. Krasnov, F. Ding, A. K. Singh, B. I. Yakobson, *J. Phys. Chem. C* **2007**, *111*, 17977-17980.

[18] Q. Sun, Q. Wang, P. Jena, Y. Kawazoe, *J. Am. Chem. Soc.* **2005**, *127*, 14582.

[19] U. Zimmerman, N. Malinowski, U. Näher, S. Frank, T. P. Martin, *Phys. Rev. Lett.* **1994**, *72*, 3542-3545.

[20] F. Tast, N. Malinowski, S. Frank, M. Heinebrodt, I. M. L. Billas, T. P. Martin, *Z. Phys. D* **1997**, *40*, 351-354.

[21] J. L. Fye, M. F. Jarrold, *Int. J. Mass. Spectrom* **1999**, *185*, 507-515.

[22] E. K. Parks, K. P. Kerns, S. J. Riley, B. J. Winter, *Phys. Rev. B* **1999**, *59*, 13431-13445.

[23] G. A. Grieves, J. W. Buchanan, J. E. Reddic, M. A. Duncan, *Int. J. Mass. Spectrom.* **2001**, *204*, 223-232.

[24] M. E. Geusic, M. D. Morse, R. E. Smalley, *J. Chem. Phys.* **1985**, *82*, 590-591.

[25] A. Nakajima, T. Kishi, Y. Sone, S. Nonose, K. Kaya, *Z. Phys. D* **1991**, *19*, 385-387.

[26] J. Niu, B. K. Rao, P. Jena, M. Manninen, *Phys. Rev. B* **1995**, *51*, 4475.

[27] H. T. Le, S. M. Lang, J. De Haeck, P. Lievens, E. Janssens, *Phys. Chem. Chem. Phys.* **2012**, *14*, 9350.

[28] G. E. Johnson, E. C. Tyo, A. W. Castleman, *Proc. Natl. Acad. Sci. U.S.A.* **2008**, *105*, 18108-13.

[29] K. García-Díez, J. Fernández-Fernández, J. A. Alonso, M. J. López, *Phys. Chem. Chem. Phys.* **2018**, *20*, 21163-21176.

[30] F. Liu, P. B. Armentrout, *J. Chem. Phys.* **2005**, *122*, 1-13.

[31] I. S. Chopra, S. Chaudhuri, J. F. Veyan, Y. J. Chabal, *Nature Mater.* **2011**, *10*, 986.

[32] R. Mendez-Camacho, R. A. Guirado-Lopez, *J. Phys. Chem. C* **2013**, *117*, 10059-10069.

[33] R. Gehrke, P. Gruene, A. Fielicke, G. Meijer, K. Reuter, *J. Chem. Phys.* **2009**, *130*, 034306.

[34] K. Hansen, *Chem. Phys. Lett.* **2015**, *620*, 43-45.

[35] P. Ferrari, J. Vanbuel, Y. Li, T.-W. Liao, E. Janssens, P. Lievens in *Gas-Phase Synth. Nanoparticles* (Ed.: Y. Huttel), Wiley-VCH, **2017**, pp. 59-78.

[36] A. Nakajima, S. Nagao, H. Takeda, T. Kurikawa, K. Kaya, *J. Chem. Phys.* **1997**, *16*, 649.

[37] S. Canulescu, J. Schou, S. F. Nielsen, *Appl. Phys. A* **2011**, *104*, 775-780.

[38] P. Ferrari, L. M. Molina, V. E. Kaydashev, J. A. Alonso, P. Lievens, E. Janssens, *Angew. Chem. Int. Ed.* **2016**, *128*, 11225-11229.

[39] E. Janssens, H. T. Le, P. Lievens, *Chem. - A Eur. J.* **2015**, *21*, 15256-15262.

[40] W. Kohn, L. J. Sham, *Phys. Rev.* **1965**, *140*, 1133.

[41] P. Giannozzi, S. Baroni, N. Bonini, M. Calandra, R. Car, C. Cavazzoni, D. Ceresoli, G. L. Chiarotti, M. Cococcioni, I. Dabo, *J. Phys. Condens. Matter* **2009**, *21*, 395502.

[42] G. Kresse, D. Joubert, *Phys. Rev. B.* **1999**, *59*, 1758-1775.

[43] P. E. Blöchl, *Phys. Rev. B.* **1994**, *50*, 17953-17979.

[44] B. Hammer, L. B. Hansen, J. K. Norkov, *Phys. Rev. B* **1999**, *59*, 7413-7421.

[45] S. Grimme, J. Anthony, S. Ehrlich, H. Krieg, *J. Chem. Phys.* **2010**, *132*, 154104.

[46] G. Makov, M. C. Payne, *Phys. Rev. B* **1995**, *51*, 4014-4022.

[47] G. Henkelman, B. P. Uberuaga, H. Jónsson, *J. Chem. Phys.* **1995**, 113, 9901-9904.

[48] D. Sheppard, R. Terrell, G. Henkelman, *J. Chem. Phys.* **2008**, 128, 134106.

10.1002/cphc.202000146

Table of Contents Entry

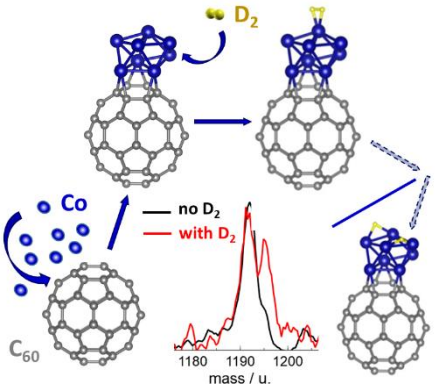

The reaction kinetics of $Co_nC_{60}^+$ (n = 1 to 8) towards deuterium has been investigated in a few-collision reaction cell. The size-dependent reactivity hints towards Co aggregation on the fullerene surface, what is confirmed by DFT calculations. The thermodynamically favorable deuterium adsorption mechanism is molecular for n = 1, 2 and dissociative for n = 3 to 8. However, dissociation barriers may hinder reaching the ground state configuration within the time scale of the experiment.